Data in Brief 40 (2022) 107823

Contents lists available at ScienceDirect

Data in Brief

journal homepage: www.elsevier.com/locate/dib

Data Article

Geochemical dataset of high-pressure acid migmatites from the Cabo Ortegal Complex (NW Spain)

Aratz Beranoaguirre[a,b,*], Sonia Garcia de Madinabeitia[b], Maria Eugenia Sanchez-Lorda[c], Pablo Puelles[b], Benito Abalos[b], Jose Ignacio Gil-Ibarguchi[b]

[a] *Institut für Geowissenschaften, Goethe-Universität, Altenhöferallee 1, Frankfurt am Main 60438, Germany*
[b] *Geologia Saila, Euskal Herriko Unibertsitatea UPV/EHU, PO Box 644, Bilbao 48080, Spain*
[c] *Geokronologia eta Geokimika Isotopikoaren Zerbitzua – SGIker-IBERCRON, Euskal Herriko Unibertsitatea UPV/EHU, PO Box 644, Bilbao 48080, Spain*

ARTICLE INFO

Article history:
Received 29 October 2021
Revised 23 December 2021
Accepted 7 January 2022
Available online 10 January 2022

Keywords:
Whole-rock geochemistry
Cabo Ortegal Complex
NW Iberia
Migmatite
Variscan

ABSTRACT

This brief note presents geochemical data from rock samples from the Cabo Ortegal Complex (NW Spain). The samples belong to acid lithologies within the mainly basic to intermediate granulite unit that have been poorly investigated so far. For this communication, five samples of the migmatites and an amphibolitic enclave within them have been analysed. The whole-rock major and trace-element analyses were accomplished by means of Q-ICPMS. The dataset provides new and useful information relevant to the origin of the acid migmatites and can be used in addition to information from neighbouring lithologies to enhance understanding of the geological evolution of the Western Variscan Belt.

* Corresponding author at: Geologia Saila, Euskal Herriko Unibertsitatea UPV/EHU, PO Box 644, Bilbao 48080, Spain.
E-mail address: aratz.beranoaguirre@ehu.eus (A. Beranoaguirre).

https://doi.org/10.1016/j.dib.2022.107823

Specifications Table

Subject	Earth Sciences
Specific subject area	Geochemistry and Petrology
Type of data	Table Figure
How data were acquired	Analysis of whole-rock composition (major and trace elements) using quadrupole ICPMS (Thermo Fisher XSeries II)
Data format	Raw and Analyzed
Parameters for data collection	The samples were collected from the poorly studied acid lithologies within the extensively investigated, mainly basic to intermediate in composition, granulite unit of the Cabo Ortegal Complex.
Description of data collection	The description of the data collection is presented in the Experimental Design, Materials, and Methods section.
Data source location	Samples storage at: University of the Basque Country UPV/EHU, Science and Technology Faculty, SGIker research facility, Leioa (Spain) Samples collected at the Cabo Ortegal Complex, Bacariza Formation (NW Iberia). See coordinates in [1].
Data accessibility	With the article
Related research article	A. Beranoaguirre, S. Garcia de Madinabeitia, M. E. Sanchez-Lorda, P. Puelles, B. Abalos, J. I. Gil Ibarguchi, U-Pb, Hf isotope and REE constraints on high-pressure acid migmatites from the Cabo Ortegal Complex (NW Spain): New evidence of short-duration metamorphism in a Variscan subduction channel, Lithos 372-373 (2020) 105,660. doi:10.1016/j.lithos.2020.105660

Value of the Data

- The data provide geochemical information to classify and characterize the acid migmatites of the granulite unit at Cabo Ortegal.
- The data can be used to better understand the petrogenesis of the rocks.
- The data can be re-used, together with additional information, to gain further insights regarding the origin and subsequent evolution of the high-pressure metamorphic nappes of the Cabo Ortegal Complex.
- The data presented in this article complement the data obtained from the previous study [1].

1. Data Description

Geochemical data from poorly known acid migmatites exposed in the Cabo Ortegal Complex (Western Variscides, NW Spain) are presented here. The migmatites, previously called granulitic orthogneisses [2], are part of the high-pressure granulite unit, tectonically placed between the eclogite and ultramafic (peridotite-pyroxenite) units [3]. Except for the so-called felsic gneiss sample and the amphibolitic enclave, all the other samples bear evidence of partial melting. Detailed petrographic information of those migmatites can be found elsewhere [1,2]. Due to the ubiquity of the mafic granulites, earlier geochemical works in the area have been focused on those lithotypes [e.g. 4], leaving aside the scarce acid migmatite outcrops. This paper intends to fill this gap on geochemical data and for that purpose, six samples from the biotite-absent muscovite bearing migmatites (samples T-4 and CO-35a), muscovite- and biotite-bearing migmatites (CO-55a), biotite-bearing migmatites lacking muscovite (CO-5b, including an amphibolitic enclave), and mica-lacking felsic gneisses (CO-49) have been studied. Accompanying frequent minerals include garnet, quartz, feldspars and rutile, and, in some cases zoisite/clinozoisite, kyanite and antiperthitic plagioclase.

Table 1 shows the results of the whole rock major and trace element analyses of the selected samples, together with two samples from the literature [4] used in Fig. 1 (see below) for comparative purposes. All samples analysed are quite evolved, with SiO_2 contents varying from 50.2%

Table 1
Major and trace element analyses of acid migmatites from the Cabo Ortegal Complex. * from [4].

Sample	CO-08-5b	CO-08-5b$_{Enc}$	CO-35a	CO-49	CO-55a	T-4	AMP-463*	AMP-466*
Major elements (%)								
SiO_2	58.06	52.17	56.22	59.68	50.21	71.83	43.60	46.10
TiO_2	1.31	1.26	1.02	0.58	1.69	0.48	1.96	3.90
Al_2O_3	17.72	16.88	18.67	15.93	20.19	13.12	15.20	13.80
Fe_2O_3	9.18	10.98	9.73	9.50	12.86	5.12	18.20	15.80
MnO	0.17	0.12	0.16	0.19	0.24	0.11	0.24	0.28
MgO	3.78	6.67	3.08	2.34	4.57	1.10	6.5	6.22
CaO	3.56	6.56	4.47	7.81	4.46	2.57	10.9	10.8
Na_2O	3.15	2.34	3.04	3.28	3.66	1.99	1.23	0.99
K_2O	1.85	1.46	3.11	3.28	3.66	2.52	0.18	0.34
P_2O_5	0.21	0.13	0.11	0.10	0.12	0.12	0.05	0.47
LOI	0.58	0.98	0.66	0.11	0.76	0.82	0.00	0.50
Total	99.57	99.55	100.27	102.79	102.41	99.78	98.06	99.20
Trace elements (ppm)								
Sc	23.5	25.9	4.53	4.84	4.15	24.9	-	-
V	139.1	228.1	171.6	124.5	268.9	35	-	-
Cr	85.3	280.0	158.6	204.9	211.9	54.3	200	300
Co	19.0	96.1	34.77	19.61	70.61	75.2	55	36
Ni	47.0	82.4	46.97	b.d.l.	218.2	6.1	b.d.l.	55
Cu	45.1	46.2	21.9	15.64	21.01	b.d.l.	-	-
Zn	54.6	125.4	56.92	55.92	91.11	38.1	-	-
Rb	54.0	32.9	109.8	7.782	69.42	54.4	4	7
Sr	197.9	120.6	201.7	280.1	265.9	151	153	62
Y	35.1	35.8	35.08	19.77	68.37	100	b.d.l.	46
Zr	194.1	124.4	231.3	57.58	380.9	401.2	37	235
Nb	9.2	6.1	13.23	b.d.l.	25.29	10	5	7
Ba	488.7	258.7	780.3	75.72	491.8	915	167	252
La	20.5	15.0	38.07	9.229	86.56	111	2	10.7
Ce	55.6	33.7	95.3	17.43	176.5	229	5	28
Pr	5.9	4.2	11.46	2.631	23.65	29.4	-	-
Nd	22.5	18.0	44.11	11.61	93.56	114	4	21
Sm	5.2	5.4	9.179	3.059	18.8	23.3	1.17	6.61
Eu	1.2	1.5	2.157	1.316	3.473	2.7	0.69	2.66
Gd	5.2	6.4	11.28	3.668	23.34	19.5	-	-
Tb	0.9	1.1	1.372	0.605	2.727	3.03	0.3	1.7
Dy	6.1	6.6	7.525	3.636	14.79	18.5	1.9	10
Ho	1.0	1.1	1.498	0.779	3.041	3.11	-	-
Er	3.4	3.5	4.465	2.322	9.17	10.3	-	-
Tm	0.6	0.6	0.652	0.366	1.367	1.71	-	-
Yb	3.6	3.5	4.428	2.535	9.031	10.1	1.24	5.75
Lu	0.6	0.6	0.628	0.388	1.24	1.79	0.19	0.86
Hf	5.7	3.9	6.574	1.699	10.76	12.75	1	7
Ta	0.8	1.0	1.001	0.194	1.962	1.25	b.d.l.	b.d.l.
Th	9.1	3.9	8.723	1.405	18.15	28.3	b.d.l.	b.d.l.
U	1.3	1.0	2.16	1.181	2.242	2.4	0.2	0.4

up to 71.8% and MgO <5%, except for the amphibolite nodule in sample CO-5b. Their freshness is confirmed by the < 1% values for loss on ignition.

Harker diagrams for major element oxides are presented in Fig. 1. As a comparison, we also plotted the geochemical data of two already published data of mafic and rare ultramafic (pyri-garnite) granulites within the same unit (from [4]). All major elements except K_2O exhibit a coherent decreasing linear trend with respect to increasing SiO_2, above all observable in MgO and Fe_2O_3 diagrams. This is consistent with a differentiation process for magmatic protoliths of the granulite unit. The main difference between mafic and acid rocks is related to the higher alkali (Na_2O and K_2O) contents as well as distinctively lower Fe_2O_3 and CaO components in the latter. Indeed, the amount of K_2O in acid lithotypes is responsible for the characteristic white mica growth in the migmatites. Regarding the trace elements, the most significant feature is the

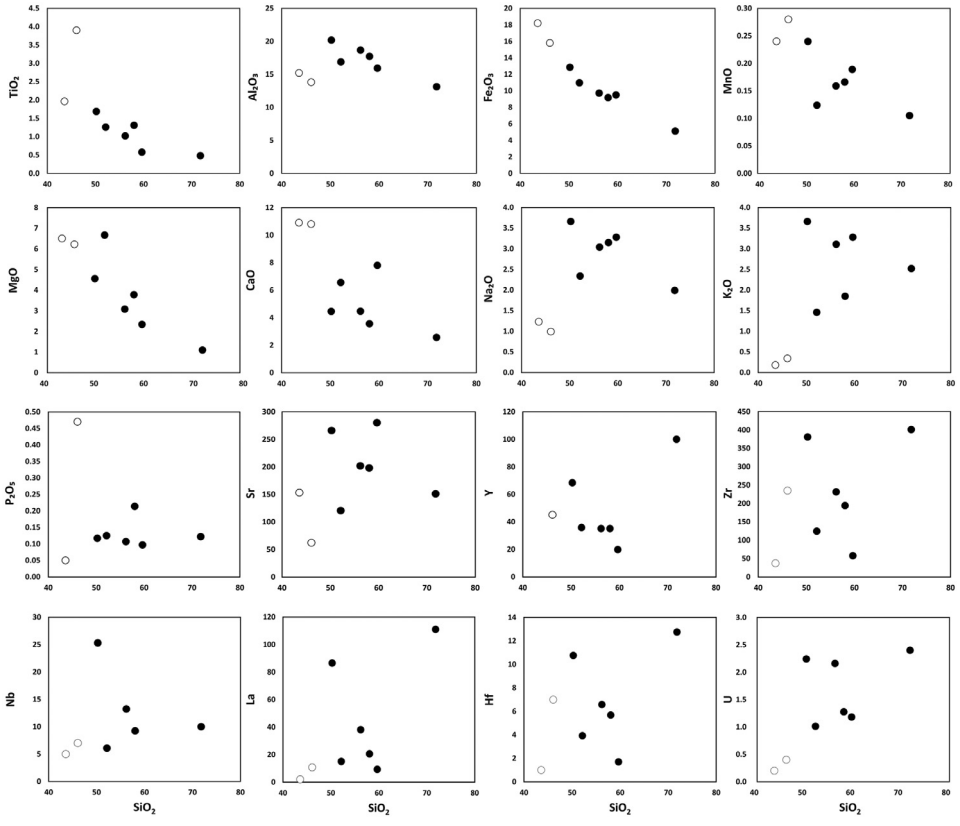

Fig. 1. Plots of SiO_2 content against different major elements oxide (Harker diagram) of the samples. Black dots correspond to the samples analysed here, white dots are from [4]. See text for further explanations.

increasing of U content increasing SiO_2. It is also worth mentioning the low Zr and Hf content on the mica-lacking gneisses (sample CO-49), where lower amount of zircon was also observed. Likewise, the gneisses have a distinctive lower content of REE in comparison to the amount observed in the white mica rich lithotypes (ΣREE $<$ 60 µg/g in the gneisses against ΣREE $>$ 550 µg/g in the biotite-absent muscovite bearing migmatite, sample T-4).

According to the classification of [5] (Fig. 2a), the migmatite samples are peraluminous, except for the amphibolite enclave in sample CO-5b that plots in the metaluminous field. When plotting in the ternary AFM diagram of [6] (Fig. 2b) the samples show a calc-alkaline affinity but close to the boundary with the tholeiitic series. The rocks studied here do not plot in any particular field of the ones proposed by [7] (Fig. 2c), pointing to a progressive trend. Similarly, the tectonic discrimination diagrams of [8] are also inconclusive (Fig. 2d), with cases straddling the boundaries between volcanic-arc and within-plate granites.

Trace element concentrations (Table 1) are reported in primitive mantle-normalized multi-element diagrams and chondrite-normalized REE patterns (Fig. 3, normalized to [9]). They display patterns typical for volcanic-arc scenarios, with enrichments in large-ion lithophile elements (Rb, Ba) and depletion in Nb and Ta (Fig. 3a), as well as enrichment in LREE (La, Ce, Pr) over HREE (Fig. 3b). A notable feature of these patterns is their negative anomaly in Sr and Eu in the partially melted samples, i.e. all except the felsic gneiss, which is slightly enriched in Sr and Eu. This reflects the more evolved nature of the samples because Sr becomes relatively depleted with respect to its neighbouring elements during plagioclase fractionation. Indeed, the

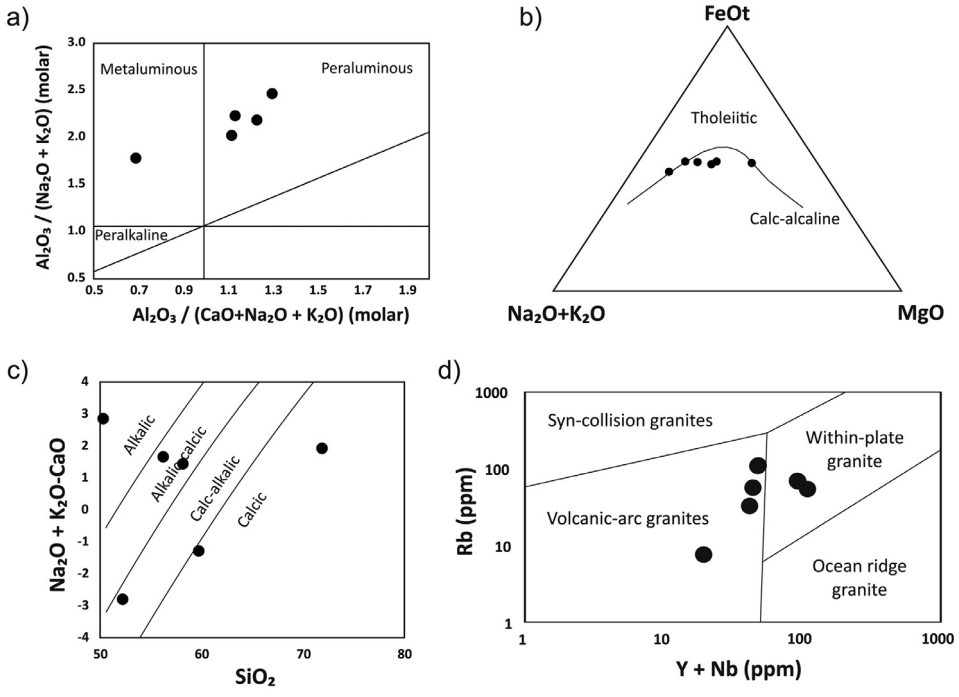

Fig. 2. Samples of the acid migmatites plotted in classification diagrams proposed by (a) [5], (b) [6], (c) [7], and (d) [8].

positive anomaly in Sr and Eu observed in the felsic gneisses may indicate the cumulative nature of this lithology.

2. Experimental Design, Materials and Methods

The sample processing was accomplished at the sample preparation laboratories of the Geology Department at the University of the Basque Country UPV/EHU. 5 to 10 kgs of the sample (depending on grain size) were ground using first a jaw crusher (Retsch bb200 Wolframcarbid) and subsequently a Retsch RS1 type ring-mill with widia rings.

The measurement protocol was mostly based on the procedures of [10], and it was as follows: 250 mg of sample and 500 mg of $LiBO_2$ were put into the Pt(Au) crucible with three to four drops of LiBr solution as a non-wetting agent. The mixture was fused and poured onto a polypropylene beaker containing 100 ml of diluted HNO3:HF acid mixture. The solution was stirred ca. 10 min to ensure total dissolution. The samples were consequently analysed using a Thermo Fisher XSeriesII quadrupole ICPMS at the SGIker Research Facilities of the University of the Basque Country UPV/EHU. The precision for all analytes is in general $< 2\%$. The LOI was determined by heating the samples using a muffle furnace with a temperature of 1000 °C. Before and after heating the samples, their masses were measured using a balance weighing with the accuracy ± 0.0002 g so the weight loss was used to calculate the LOI.

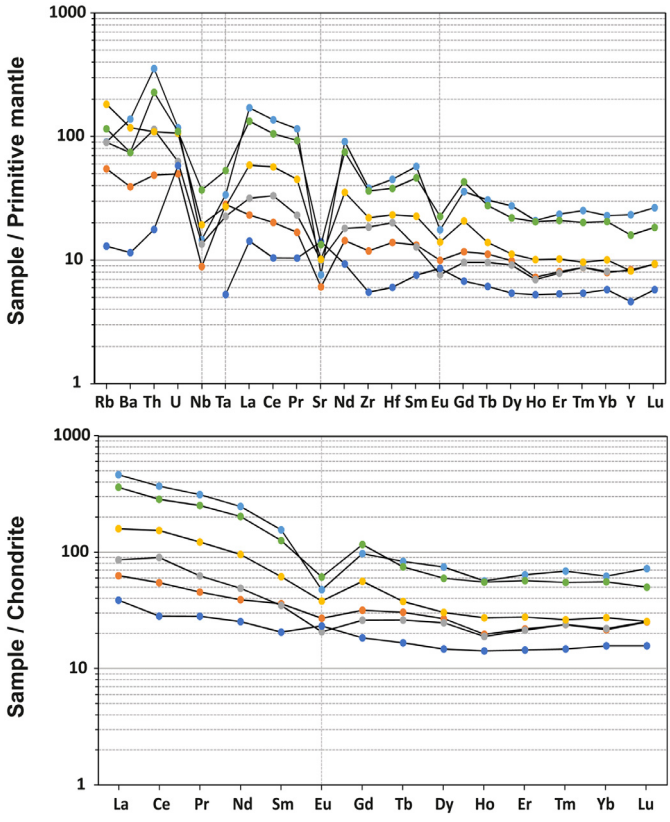

Fig. 3. Multi-element and REE patterns of the studied samples. Normalization values are the 'pyrolite silicate Earth' for the primitive mantle, and C1 chondrites [9].

Ethics Statement

Not applicable.

Declaration of Competing Interest

The authors declare that they have no known competing financial interests or personal relationships which have, or could be perceived to have, influenced the work reported in this article.

CRediT Author Statement

Aratz Beranoaguirre: Investigation, Formal analysis, Data curation, Writing – original draft; **Sonia Garcia de Madinabeitia:** Formal analysis, Writing – original draft; **Maria Eugenia Sanchez-Lorda:** Formal analysis, Writing – original draft; **Pablo Puelles:** Data curation, Writing – original draft; **Benito Abalos:** Data curation, Writing – original draft; **Jose Ignacio Gil-Ibarguchi:** Data curation, Writing – original draft.

Acknowledgments

Financial support was provided by the Basque Country University UPV/EHU (Project GIU20/10). Technical and human support provided by the Geochronology and Isotope Geochemistry and the Electronic Microscopy and Material Microanalysis SGIker facilities (UPV/EHU, MINECO, GV/EJ, ERDF and ESF) is acknowledged.

References

[1] A. Beranoaguirre, S. Garcia de Madinabeitia, M.E. Sanchez-Lorda, P. Puelles, B. Abalos, J.I. Gil Ibarguchi, U-Pb, Hf isotope and REE constraints on high-pressure acid migmatites from the Cabo Ortegal Complex (NW Spain): new evidence of short-duration metamorphism in a Variscan subduction channel, Lithos 372-373 (2020) 105660, doi:10.1016/j.lithos.2020.105660.

[2] P. Puelles, B. Ábalos, J.I. Gil Ibarguchi, Metamorphic evolution and thermobaric structure of the subduction-related Bacariza high-pressure granulite formation (Cabo Ortegal Complex, NW Spain), Lithos 84 (2005) 125–149, doi:10.1016/j.lithos.2005.01.009.

[3] J.R. Martínez Catalán, J. Gómez Barreiro, I. Dias da Silva, M. Chichorro, A. López-Carmona, P. Castiñeiras, J. Abati, P. Andonaegui, J. Fernández-Suárez, P. González Cuadra, J.M. Benítez-Pérez, C. Quesada, J.T. Oliveira, Variscan suture zone and suspect terranes in the NW Iberian massif: allochthonous complexes of the Galicia-Trás os Montes Zone (NW Iberia), in: The Geology of Iberia: A Geodynamic Approach. Volume 2: The Variscan Cycle. Regional Geology Reviews, Springer, 2019, pp. 99–130, doi:10.1007/978-3-030-10519-8_4.

[4] G. Galan, A. Marcos, Geochemical evolution of high-pressure mafic granulites from the Bacariza formation (Cabo Ortegal Complex, NW Spain): an example of a heterogeneous lower crust, Geol. Rundsch. 86 (1997) 539–555, doi:10.1007/s005310050162.

[5] P.D. Maniar, P.M. Piccoli, Tectonic discrimination of granitoids, Geol. Soc. Am. Bull. 101 (1989) 635–643, doi:10.1130/0016-7606(1989)101⟨0635:TDOG⟩2.3.CO;2.

[6] T.N. Irvine, W.R.A. Baragar, A guide to the chemical classification of the common volcanic rocks, Can. J. Earth Sci. 8 (1971) 523–548, doi:10.1139/e71-055.

[7] B.R. Frost, C.G. Barnes, W.J. Collins, R.J. Arculus, D.J. Ellis, C.D. Frost, A geochemical classification for granitic rocks, J. Petrol. 42 (2001) 2033–2048, doi:10.1093/petrology/42.11.2033.

[8] J.A. Pearce, N.B.W. Harris, A.G. Tindle, Trace element discrimination diagrams for the tectonic interpretation of granitic rocks, J. Petrol. 25 (1984) 956–983, doi:10.1093/petrology/25.4.956.

[9] W.F. McDonough, S.S. Sun, The composition of the earth, Chem. Geol. 120 (1995) 223–253, doi:10.1016/0009-2541(94)00140-4.

[10] S. Garcia de Madinabeitia, M.E. Sanchez-Lorda, J.I. Gil Ibarguchi, Simultaneous determination of major to ultratrace elements in geological samples by fusion-dissolution and inductively coupled plasma mass spectrometry techniques, Anal. Chim. Acta 625 (2008) 117–130, doi:10.1016/j.aca.2008.07.024.